

DOI: 10.1002/adma.((please add manuscript number))

Interface control of ferroelectricity in a SrRuO₃/BaTiO₃/SrRuO₃ capacitor and its critical thickness

Yeong Jae Shin, Yoonkoo Kim, Sung-Jin Kang, Ho-Hyun Nahm, Pattukkannu Murugavel, Jeong Rae Kim, Myung Rae Cho, Lingfei Wang, Sang Mo Yang, Jong-Gul Yoon, Jin-Seok Chung, Miyoung Kim, Hua Zhou, Seo Hyoung Chang, Tae Won Noh**

Y. J. Shin, Dr. S.-J. Kang, Dr. H.-H. Nahm, J. R. Kim, Dr. M. R. Cho, Dr. L. Wang, Prof. T. W. Noh

Center for Correlated Electron Systems, Institute for Basic Science (IBS), Seoul 08826, Republic of Korea

Department of Physics and Astronomy, Seoul National University, Seoul 08826, Republic of Korea

E-mail: twnoh@snu.ac.kr

Y. Kim, Prof. M. Kim

This is the author manuscript accepted for publication and has undergone full peer review but has not been through the copyediting, typesetting, pagination and proofreading process, which may lead to differences between this version and the [Version of Record](#). Please cite this article as [doi: 10.1002/adma.201602795](https://doi.org/10.1002/adma.201602795).

This article is protected by copyright. All rights reserved.

Department of Materials Science and Engineering and Research Institute of Advanced Materials, Seoul National University, Seoul 08826, Republic of Korea

Prof. P. Murugavel

Department of Physics, Indian Institute of Technology Madras, Chennai 600036, India

Prof. S. M. Yang

Department of Physics, Sookmyung Women's University, Seoul 04310, Republic of Korea

Prof. J.-G. Yoon

Department of Physics, University of Suwon, Hwaseong, Gyeonggi-do 18323, Republic of Korea

Prof. J.-S. Chung

Department of Physics, Soongsil University, Seoul 06978, Republic of Korea

Dr. H. Zhou

Advanced Photon Source, Argonne National Laboratory, Lemont, Illinois 60439, United States

Prof. S. H. Chang

Department of Physics, Pukyong National University, Busan 48513, Republic of Korea

E-mail: cshyoung@pknu.ac.kr

Keywords: Interface engineering, ferroelectric critical thickness, ferroelectricity, BaTiO₃

The atomic-scale synthesis of artificial oxide heterostructures offers new opportunities to create novel states that do not occur in nature. The main challenge related to synthesizing these structures is obtaining atomically sharp interfaces with designed termination sequences.^[1,2] Here, we demonstrate that the oxygen pressure (P_{O_2}) during growth plays an important role in controlling the interfacial terminations of SrRuO₃/BaTiO₃/SrRuO₃ (SRO/BTO/SRO) ferroelectric capacitors. The SRO/BTO/SRO heterostructures were grown by the pulsed laser deposition (PLD) method. The top SRO/BTO interface grown at high P_{O_2} (around 150 mTorr) usually exhibited a mixture of RuO₂-BaO and SrO-TiO₂ terminations. By reducing P_{O_2} , we obtained atomically sharp SRO/BTO top interfaces with uniform SrO-TiO₂ termination. Using capacitor devices with symmetric and uniform interfacial termination, we were able to demonstrate for the first time that the ferroelectric (FE) critical thickness can reach the theoretical limit of 3.5 unit cells (u.c.).^[3]

Oxide heterostructures have attracted significant research interest due to the discovery of novel emergent phenomena.^[2,4-13] As a result, heteroepitaxy growth techniques have advanced significantly during the last two decades. However, the task of

This article is protected by copyright. All rights reserved.

realizing high-quality oxide heterostructures with atomically sharp interfaces is still challenging, even for simple perovskite oxides. For instance, it has been widely accepted that each maximum of a reflective high-energy electron diffraction (RHEED) intensity profile during PLD growth corresponds to the growth of one unit cell. The perovskite stacking sequence is therefore expected to be preserved during stoichiometric deposition (i.e. a *unit-cell-by-unit-cell* growth scheme). However, recent studies have shown that RHEED oscillations alone do not provide sufficient information to confirm the intended atomic structure of the surface.^[14–16] During PLD growth, numerous growth variables, including the chemical stabilities and mobilities of surface adatoms, can be altered by the growth conditions. This alternation may in turn give rise to uncontrollable changes of surface termination.^[15,16] Up to this point, there have been few investigations on how the key growth parameters, e.g. P_{O_2} and temperature, affect the surface termination.

Ultrathin FE heterostructures are model systems in which the physical properties are highly dependent on the interfacial structure. As the FE film thickness decreases, the FE polarization decreases monotonically and finally disappears at a critical thickness. According to theoretical predictions, the prototypical all-oxide SRO/BTO/SRO

This article is protected by copyright. All rights reserved.

heterostructure should have a critical thickness between 3.5 – 6.5 u.c..^[3,17] Experimental critical thicknesses are, however, significantly larger. Recent studies on SRO/BTO/SRO capacitors have shown that the lack of atomic scale interface control is the main obstacle to obtaining FE critical thicknesses approaching the theoretical limit.^[18,19] The experimental structures feature mixed terminations and the resulting pinned dipoles notably degrade the FE polarization stability, which results in the suppression of ferroelectric behavior below about 20 u.c..^[19]

Here, we demonstrate the critical role of P_{O_2} in determining the interface termination. Using scanning transmission electron microscopy (STEM) and x-ray diffraction, the interfaces of SRO/BTO heterostructures were studied for various $P_{O_2} = 5$ and 150 mTorr. In the 150 mTorr case, we found a mixed interfacial termination. However, for $P_{O_2} = 5$ mTorr, a singly terminated interface was observed. Our density functional theory (DFT) calculations also support that the stability of the possible interface atomic structures are significantly affected by changing P_{O_2} . Capacitor devices grown at $P_{O_2} = 5$ mTorr with well-controlled interfaces show FE critical thicknesses as low as 3.5 u.c., in agreement with theory.^[3]

This article is protected by copyright. All rights reserved.

The SRO/BTO/SRO capacitor can have two possible atomic arrangements, as illustrated in **Scheme 1**. Since RuO_2 is thermally unstable during high-temperature deposition, the bottom SRO layer is always SrO terminated.^[16] The BTO layer, therefore, starts with TiO_2 . Following the commonly assumed *unit-cell-by-unit-cell growth* mode, the growth of the BTO layer should end with a top BaO termination. As a result, the top interface should have the sequence BaO- RuO_2 , which produces an asymmetric capacitor configuration (Scheme 1b). On the other hand, the FE critical thickness calculations have been performed only for ideal symmetric configurations with TiO_2 termination on both top and bottom BTO surfaces (Scheme 1a).^[3,17] Obtaining such a symmetric termination configuration is essential to test the theoretically predicted value of the FE critical thickness.

Fully strained SRO/BTO/SRO heterostructures were fabricated using PLD on atomically smooth TiO_2 -terminated $\text{SrTiO}_3(001)$ substrates. The thicknesses of the bottom and top SRO electrodes were fixed at 20 nm. During the BTO growth, P_{O_2} was set to either 5 or 150 mTorr. The BTO film thickness (t_{BTO}) was controlled by monitoring the high pressure RHEED intensity oscillations. In the ideal layer-by-layer growth mode, the

This article is protected by copyright. All rights reserved.

number (n) of RHEED oscillations signifies a BTO layer with thickness $t_{\text{BTO}} = n$ u.c..

However, by using STEM, we found that the films grown at $P_{\text{O}_2} = 5$ mTorr end with a half-unit-cell BTO layer (Figure S1, Supporting Information). In this case, we denote the film thickness by $t_{\text{BTO}} = (n-0.5)$ u.c.. Using x-ray diffraction (Figure S2, Supporting Information), we exclude the formation of secondary phases for both growth conditions ($P_{\text{O}_2} = 150$ and 5 mTorr).

For $P_{\text{O}_2} = 150$ mTorr, we found that two types of termination sequence coexist at the top SRO/BTO interface. **Figure 1a** shows a cross-sectional high-angle annular dark field (HAADF) image from STEM, viewed along the [100] zone axis. The HAADF image displays an atomically sharp BTO/SRO bottom interface with the expected TiO_2 -SrO termination sequence. By contrast, the SRO/BTO top interface termination is highly inhomogeneous. Figure 1b and 1c presents the magnified HAADF images for two regions marked in Figure 1a (dashed boxes I and II). The intensity profiles along the B-site cations are also plotted in the right panels. Note that the intensity of the Ti peaks is lower than those of the Ru peaks due to the smaller atomic number. Four (three) TiO_2 layers imply that the BTO film thickness is 3.5 u.c. (3 u.c.), and the resulting SrO- TiO_2

This article is protected by copyright. All rights reserved.

(RuO₂-BaO) interface will produce a symmetric (asymmetric) capacitor configuration. The mixed termination sequence of the top surface was confirmed by STEM images of different regions of the sample (Figure S3 in the Supporting Information).

In the SRO/BTO/SRO capacitor with mixed interfacial termination, the local FE response varies significantly. Using the electron-beam lithography technique, we fabricated a 5 × 5 μm² square-shaped capacitor (see Experimental Section). We then chose 10×10 grid positions on the SRO top electrode layer and characterized the local FE responses at each grid point by piezoresponse force microscopy (PFM) (See Figure S4 in the Supporting Information for details).^[20] As shown in Figure 1d, we can observe two typical piezoresponse signals. In region (i) (left panel), the PFM phase-voltage curve shows a fully saturated hysteresis and the PFM amplitude-voltage curve has a nearly symmetric butterfly shape, indicating robust and switchable ferroelectricity. In region (ii) (right panel), by contrast, the PFM amplitude and phase show FE polarization switching characteristics only for the downward polarization state (pointing towards the bottom SRO). This result implies that the FE polarization in the region (ii) is strongly pinned

This article is protected by copyright. All rights reserved.

along one direction. The existence of pinned dipoles in the mixed terminated

SRO/BTO/SRO capacitor was also proposed by earlier works.^[18,19,21]

In order to map the spatial variation of the ferroelectricity, we calculated the ratio between the PFM amplitudes at ± 6 V (A_{+max}/A_{-max}) at each sampling point. As shown in the central panel of Figure 1d, for approximately 50% of points the A_{+max}/A_{-max} ratio is close to 1.0, signifying switchable FE response [region (i)]. For the remaining points, A_{+max}/A_{-max} is much higher than 1.0, signifying the response of pinned dipoles [region (ii)]. It is therefore difficult to test the FE critical thickness experimentally with the SRO/BTO/SRO capacitors grown at $P_{O_2} = 150$ mTorr.

In contrast, the heterostructure grown at $P_{O_2} = 5$ mTorr has a uniform BTO top interface and a symmetric termination sequence (Scheme 1a). As shown in **Figure 2a** and **2b**, the high-resolution HAADF images reveal atomically sharp interfaces formed over a lateral range of 40 nm. The BTO layer is uniformly TiO_2 -terminated for both the top and bottom interfaces. The intensity profile along the solid box in Figure 2b also confirms the symmetric SrO- TiO_2 interface termination sequences (Figure 2c). In this sample with alternatively stacked 3 BaO and 4 TiO_2 layers, we denote the t_{BTO} as 3.5 u.c (Figure 2d).

This article is protected by copyright. All rights reserved.

Considering that the STEM images only provide local structural information, we also performed surface x-ray scattering measurements and a coherent Bragg rod analysis (COBRA) to further confirm the uniformity of the BTO interfaces.^[22] The sample used for this measurement contains a 5 mTorr grown BTO layer (3.5 u.c.) sandwiched between two SRO layers (3 u.c. each). The COBRA electron density mapping (Figure 2e) indicates that the symmetric SrO-TiO₂ interface termination occurs uniformly over the size of the x-ray beam spot, which is typically 30 μm in diameter. These structural investigations clearly indicate that the heterostructure grown with $P_{O_2} = 5$ mTorr has a uniformly TiO₂-terminated interface.

We now turn to possible interpretations of the observed P_{O_2} -dependent termination change. We first checked the cation stoichiometry of the BTO films. Some earlier studies showed that different background pressures could change the composition or stoichiometry of BTO during the growth.^[23–25] However, STEM-energy dispersive spectroscopy confirms that our films grown at different P_{O_2} are close to stoichiometric with the Ti/Ba ratio very close to one (Figure S5, Supporting information). To check the oxygen stoichiometry, we evaluated the lattice constant of the BTO layer

This article is protected by copyright. All rights reserved.

with $P_{O_2} = 5$ mTorr from the COBRA electron density map. The measured c -axis lattice constant was quite consistent with that of a fully strained BTO film on a $SrTiO_3$ (001) substrate. This indicates that there is no significant amount of oxygen vacancies in our BTO layer even with a lower P_{O_2} condition. Therefore, we exclude the possibility that deviations in film stoichiometry play a significant role in affecting the composition of the BTO surface and interface termination.

Another possible interpretation is that the P_{O_2} dependent termination could be related to the stability of BaO and TiO_2 terminations during the growth. The stability of each component can play an important factor in determining the interface terminations. A typical example is epitaxial SRO film growth on $SrTiO_3$ (001) substrates. It is already widely known that termination conversion can occur during the growth of epitaxial SRO films.^[16,26-28] The highly volatile nature of RuO_2 makes the RuO_2 -termination unstable during the high-temperature growth, leading to a conversion to SrO-termination. In the BTO case, the stabilities of possible surface structures were reported to be strongly dependent on the background oxygen pressure.^[29,30] A change in relative stability may also act as a driving force for forming different surface terminations of BTO. To shed

This article is protected by copyright. All rights reserved.

light on this idea, we performed DFT calculations on the Gibbs free energies of BaO- and TiO₂-terminated BTO surface (Section VI, Supporting Information). The DFT calculations showed that the TiO₂ termination becomes more stable with decreasing P_{O_2} (Figure S6, Supporting Information). This is qualitatively consistent with our experimental observations. The change of stability may imply a different bonding strength for each termination which may in turn affect the actual kinetic growth process of PLD and ultimately the termination. Nonetheless, the non-equilibrium nature of PLD makes connecting the DFT results with our experiment challenging. Additional factors that could also affect the surface termination include the density of excited arrived species and surface/arrived species interactions. Further study of the exact mechanism that determines the surface termination is therefore required.

Using BTO capacitors with symmetric interfaces, we investigated the FE critical thickness and experimentally confirmed a robust FE response down to $t_{BTO} = 3.5$ u.c.. We performed PFM hysteresis loop measurements at 10×10 grid points on a capacitor with 5 × 5 μm² sizes. **Figure 3a** displays the calculated A_{+max}/A_{-max} ratio of PFM loops measured at each grid point for a $t_{BTO} = 3.5$ u.c. capacitor. The local variation of the FE response is

This article is protected by copyright. All rights reserved.

much smaller than in the sample with mixed BTO termination. For the majority of points, the A_{+max}/A_{-max} values are very close to 1.0, indicating symmetric and switchable FE polarization. The averaged PFM hysteresis loops (Figure 3b) also show symmetric butterfly-shaped amplitude-voltage curves and fully saturated phase-voltage curves that are uniform within the error bar. Template matching analysis^[31] on the STEM images also shows that the Ti ions are displaced by about 0.1 Å relative to the center position of surrounding Ba ions, further supporting the polar nature of 3.5 u.c. BTO samples (Figure S7, Supporting Information). On the other hand, the FE signatures disappear for BTO capacitors with $t_{BTO} = 2.5$ u.c. (Figure 3c), meaning the FE critical thickness in our devices is 3.5 u.c.. This value is smaller than some theoretical values^[17,32] but is consistent with the DFT calculations of G. Gera *et al.*, who included charge distribution effects at the interface beyond the Thomas-Fermi capacitor.^[3]

In summary, we investigated the significant effect of background oxygen pressure on SRO/BTO interface termination. We found that symmetric interfaces with uniform TiO₂-terminations are crucial for decreasing ferroelectric critical thickness in SRO/BTO/SRO heterostructures, and can only be obtained utilizing a lower oxygen

This article is protected by copyright. All rights reserved.

condition (i.e. around $P_{O_2} = 5$ mTorr). As a result, we succeeded in demonstrating the theoretically predicted critical thickness of 3.5 u.c. in a real FE capacitor.^[3] Our results suggest that termination control at the atomic scale will serve as a useful tool for exploring the emergent properties of oxide heterostructures and functional devices.

Experimental

Sample fabrication and structural characterization. The SRO/BTO/SRO heterostructures were grown using the PLD technique on SrTiO₃ (001) substrates with a miscut angle of less than 0.1°. A KrF excimer laser (248 nm, COMPex pro, Coherent) was used to ablate the SRO or BTO ceramic targets. The deposition temperature was maintained at 700 °C during the entire growth process. BTO epitaxial films were grown under P_{O_2} conditions of 5 mTorr and 150 mTorr. SRO top and bottom films were grown under P_{O_2} conditions of 100 mTorr.

This article is protected by copyright. All rights reserved.

The high quality of the films was confirmed using a scanning transmission electron microscope (JEM-ARM200F, JEOL). The structure of the samples was investigated by surface x-ray scattering measurements and coherent Bragg rod analysis (COBRA) performed using Huber six-circle diffractometers at Sector 12ID-D of the Advanced Photon Source (APS) and at Sector 9C of the Pohang Light Source (PLS). For the electrical measurements of the BTO layer, capacitor devices with diameters from 500 nm to 10 μm were fabricated using e-beam lithography and ion milling.

PFM measurements. The ferroelectric polarization switching properties were measured using an atomic force microscopy (AFM) system (Cypher Asylum) at room temperature. A commercially available Cr/Pt-coated probe tip with a spring constant of ~ 40 N/m and a resonant frequency of ~ 400 kHz (Tap300E, Budget Sensors) was used. The contact resonance frequency was 1.2 – 1.3 MHz. The high spring constant and contact resonance frequency minimized possible effects of non-piezoelectric response, such as electrostatic force.^[33,34]

This article is protected by copyright. All rights reserved.

Acknowledgements

This work was supported by IBS-R009-D1 through the Research Center Program of the Institute for Basic Science in Korea. S.H.C. was supported by Basic Science Research Programs through the National Research Foundation of Korea (NRF-2015R1C1A1A01053163). Use of Advanced Photon Source was supported by the U.S. Department of Energy, Office of Science, Office of Basic Energy Sciences, under Contract No. DE-AC02-06CH11357. ((Supporting Information is available online from Wiley InterScience or from the author)).

Received: ((will be filled in by the editorial staff))

Revised: ((will be filled in by the editorial staff))

Published online: ((will be filled in by the editorial staff))

- [1] N. Nakagawa, H. Y. Hwang, D. A. Muller, *Nat. Mater.* **2006**, *5*, 204.
- [2] H. Y. Hwang, Y. Iwasa, M. Kawasaki, B. Keimer, N. Nagaosa, Y. Tokura, *Nat. Mater.* **2012**, *11*, 103.
- [3] G. Gerra, A. K. Tagantsev, N. Setter, K. Parlinski, *Phys. Rev. Lett.* **2006**, *96*, 107603.
- [4] J. Heber, *Nature* **2009**, *459*, 28.
- [5] J. Mannhart, D. G. Schlom, *Science* **2010**, *327*, 1607.
- [6] P. Zubko, S. Gariglio, M. Gabay, P. Ghosez, J.-M. Triscone, *Annu. Rev. Condens. Matter Phys.* **2011**, *2*, 141.
- [7] J. Chakhalian, A. J. Millis, J. Rondinelli, *Nat. Mater.* **2012**, *11*, 92.
- [8] A. Ohtomo, H. Y. Hwang, *Nature* **2004**, *427*, 423.
- [9] M. Huijben, A. Brinkman, G. Koster, G. Rijnders, H. Hilgenkamp, D. H. a Blank, *Adv. Mater.* **2009**, *21*, 1665.
- [10] H. Chen, A. M. Kolpak, S. Ismail-Beigi, *Adv. Mater.* **2010**, *22*, 2881.

- [11] N. Reyren, S. Thiel, A. D. Caviglia, L. F. Kourkoutis, G. Hammerl, C. Richter, C. W. Schneider, T. Kopp, A.-S. Ruetschi, D. Jaccard, M. Gabay, D. A. Muller, J.-M. Triscone, J. Mannhart, *Science* **2007**, *317*, 1196.
- [12] Y. Kozuka, M. Kim, C. Bell, B. G. Kim, Y. Hikita, H. Y. Hwang, *Nature* **2009**, *462*, 487.
- [13] A. K. Yadav, C. T. Nelson, S. L. Hsu, Z. Hong, J. D. Clarkson, C. M. Schlepüetz, A. R. Damodaran, P. Shafer, E. Arenholz, L. R. Dedon, D. Chen, A. Vishwanath, A. M. Minor, L. Q. Chen, J. F. Scott, L. W. Martin, R. Ramesh, *Nature* **2016**, *530*, 198.
- [14] J. Shin, A. Y. Borisevich, V. Meunier, J. Zhou, E. W. Plummer, S. V Kalinin, A. P. Baddorf, *ACS Nano* **2010**, *4*, 4190.
- [15] A. Tselev, R. K. Vasudevan, A. G. Gianfrancesco, L. Qiao, P. Ganesh, T. L. Meyer, H. N. Lee, M. D. Biegalski, A. P. Baddorf, S. V Kalinin, **2015**, 4316.
- [16] G. Rijnders, D. H. A. Blank, J. Choi, C.-B. Eom, *Appl. Phys. Lett.* **2004**, *84*, 505.
- [17] J. Junquera, P. Ghosez, *Nature* **2003**, *422*, 506.

- [18] X. Liu, Y. Wang, P. V. Lukashev, J. D. Burton, E. Y. Tsymbal, *Phys. Rev. B* **2012**, *85*, 125407.
- [19] H. Lu, X. Liu, J. D. Burton, C. W. Bark, Y. Wang, Y. Zhang, D. J. Kim, A. Stamm, P. Lukashev, D. A. Felker, C. M. Folkman, P. Gao, M. S. Rzechowski, X. Q. Pan, C. B. Eom, E. Y. Tsymbal, A. Gruverman, *Adv. Mater.* **2012**, *24*, 1209.
- [20] S. Jesse, A. P. Baddorf, S. V. Kalinin, *Appl. Phys. Lett.* **2006**, *88*, 21.
- [21] G. Gerra, A. K. Tagantsev, N. Setter, *Phys. Rev. Lett.* **2007**, *98*, 207601.
- [22] H. Zhou, Y. Yacoby, V. Y. Butko, G. Logvenov, I. Bozovic, R. Pindak, *Proc. Natl. Acad. Sci.* **2010**, *107*, 8103.
- [23] J. Gonzalo, C. N. Afonso, I. Madariaga, *J. Appl. Phys.* **1997**, *81*, 951.
- [24] A. P. Chen, F. Khatkhatay, W. Zhang, C. Jacob, L. Jiao, H. Wang, *J. Appl. Phys.* **2013**, *114*, 124101.
- [25] J. Gonzalo, R. Gómez San Román, J. Perrière, C. N. Afonso, R. Pérez Casero, *Appl. Phys. A Mater. Sci. Process.* **1998**, *66*, 487.

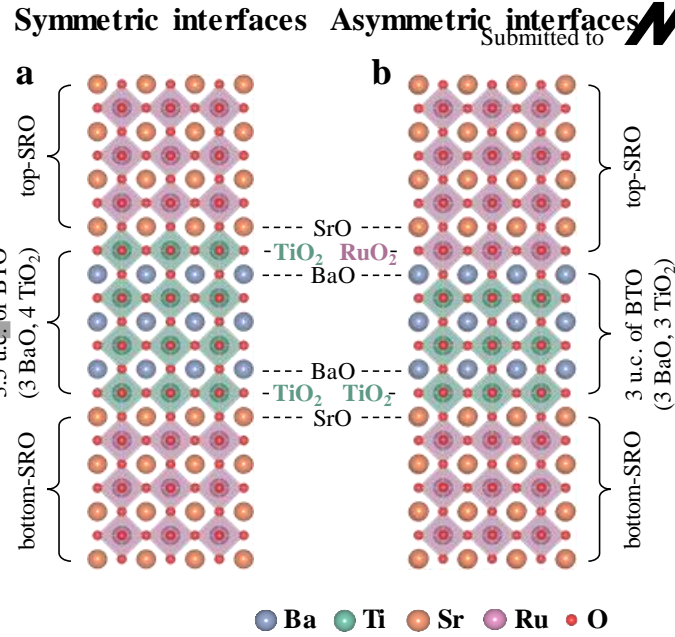
- [26] Y. J. Chang, S. H. Phark, *ACS Nano* **2016**, *10*, 5383.
- [27] P. Yu, W. Luo, D. Yi, J. X. Zhang, M. D. Rossell, C.-H. Yang, L. You, G. Singh-Bhalla, S. Y. Yang, Q. He, Q. M. Ramasse, R. Erni, L. W. Martin, Y. H. Chu, S. T. Pantelides, S. J. Pennycook, R. Ramesh, *Proc. Natl. Acad. Sci.* **2012**, *109*, 9710.
- [28] H. Yamada, A. Tsurumaki-Fukuchi, M. Kobayashi, T. Nagai, Y. Toyosaki, H. Kumigashira, A. Sawa, *Adv. Funct. Mater.* **2015**, *25*, 2708.
- [29] A. M. Kolpak, D. Li, R. Shao, A. M. Rappe, D. A. Bonnell, *Phys. Rev. Lett.* **2008**, *101*, 36102.
- [30] W. A. Saidi, J. M. P. Martirez, A. M. Rappe, *Nano Lett.* **2014**, *14*, 6711.
- [31] J. Zuo, A. B. Shah, H. Kim, Y. Meng, W. Gao, J.-L. Rouvière, *Ultramicroscopy* **2014**, *136*, 50.
- [32] B. Meyer, D. Vanderbilt, *Phys. Rev. B* **2001**, *63*, 205426.
- [33] S. Jesse, A. P. Baddorf, S. V Kalinin, *Nanotechnology* **2006**, *17*, 1615.

[34] N. Balke, P. Maksymovych, S. Jesse, A. Herklotz, A. Tselev, C. Eom, I. I. Kravchenko,

P. Yu, S. V Kalinin, *ACS Nano* **2015**, *9*, 6484.

Author Manuscript

This article is protected by copyright. All rights reserved.



Scheme 1. Schematic of the possible atomic stackings of the SrRuO₃/BaTiO₃/SrRuO₃ (SRO/BTO/SRO) heterostructure with a) symmetric SrO-TiO₂ interfaces, which result in a BTO layer thickness (t_{BTO}) of 3.5 unit cells (u.c.), and with b) BaO-RuO₂ and SrO-TiO₂ interfaces at the top and bottom of the BTO layer, respectively, which result in $t_{\text{BTO}} = 3$ u.c.. Note that the asymmetric case (b) occurs under the commonly assumed *unit-cell by unit-cell* growth mode.

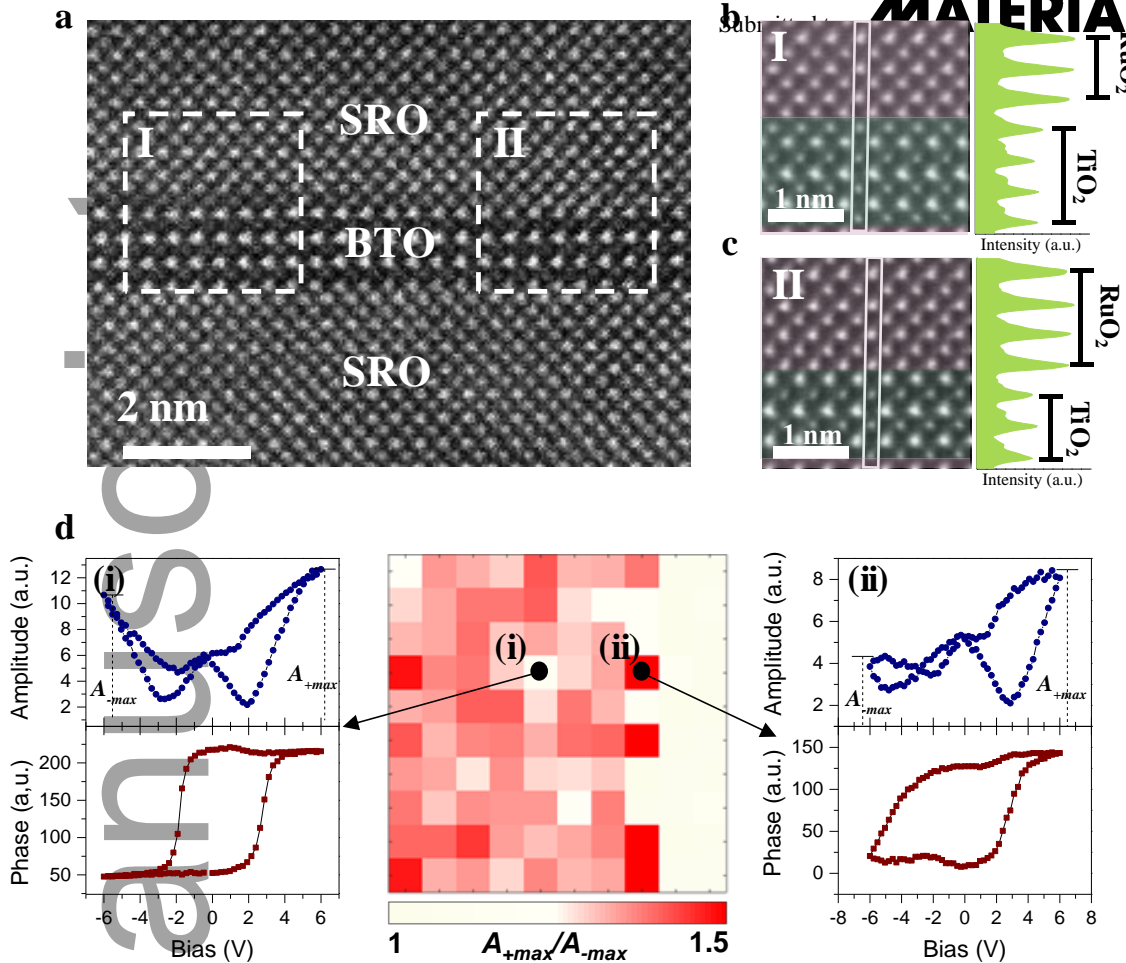


Figure 1. a) Scanning transmission electron microscopy (STEM) image of the SRO/BTO/SRO heterostructure with oxygen partial pressure (P_{O_2}) during BTO growth, equal to 150 mTorr. The magnified STEM images and intensity profiles are marked by the dashed boxes in 1a and show a mixture of b) TiO₂ and c) BaO top terminations of the BTO layer. The BTO thicknesses are 3.5 u.c. (3 BaO and 4 TiO₂) and 3 u.c. (3 BaO and 3 TiO₂) for 1b and 1c, respectively. d) The amplitude and phase from piezoresponse force microscopy (PFM) hysteresis loops collected in different locations reveal piezoresponse in both polarization directions (left) and highly pinned piezoresponse along the downward polarization direction (right). The color map at the center of 1d displays the ratio of

This article is protected by copyright. All rights reserved.

maximum PFM amplitude response (A_{+max}/A_{-max}) at positive bias (A_{+max}) to that at negative bias (A_{-max}). The black dots marked by (i) and (ii) indicate the points where the left and right plots were measured.

Author Manuscript

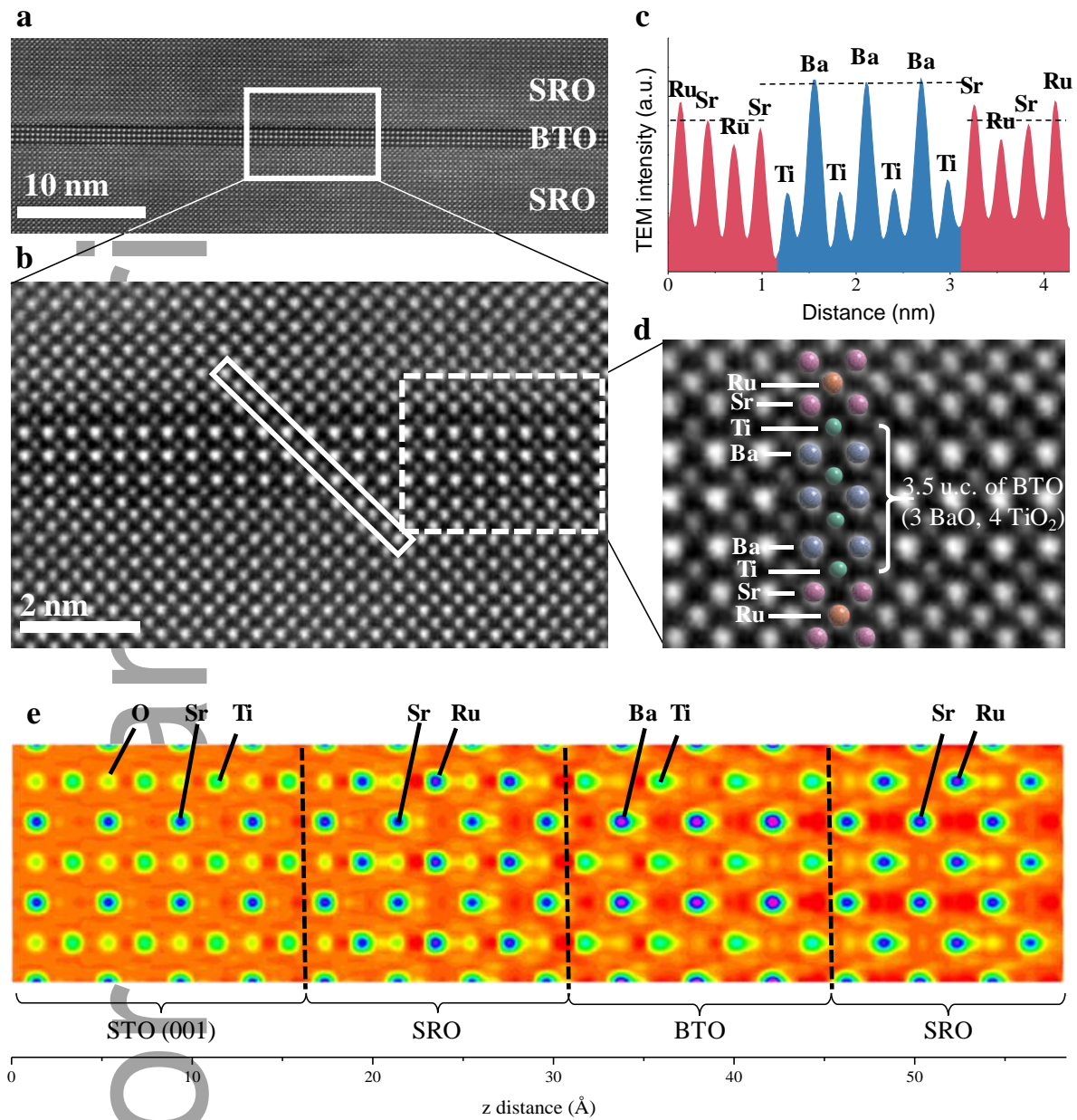


Figure 2. a) STEM image of the SRO/BTO/SRO heterostructure with $P_{O_2} = 5$ mTorr. b) Magnified STEM image of the region inside the white box in 2a. c) Intensity line profile corresponding to the highlighted solid box in 2b. This profile clearly shows the TiO_2 termination at the top and bottom of the BTO layer. d) Magnified image of the area

This article is protected by copyright. All rights reserved.

inside the white box in 2b. The different atomic species are indicated by colored circles. In the entire measured region, the BTO layer is composed of three BaO layers and four TiO₂ layers, indicating $t_{\text{BTO}} = 3.5$ u.c.. e) Coherent Bragg rod analysis (COBRA) electron density for the BTO film grown with $P_{\text{O}_2} = 5$ mTorr. The electron density map shows the (110) plane through Sr, Ba, Ti, Ru, and O. The COBRA maps show that the BTO layer has a uniform and sharp interfaces over a large length scale (i.e., at least ~ 30 μm).

Author Manuscript

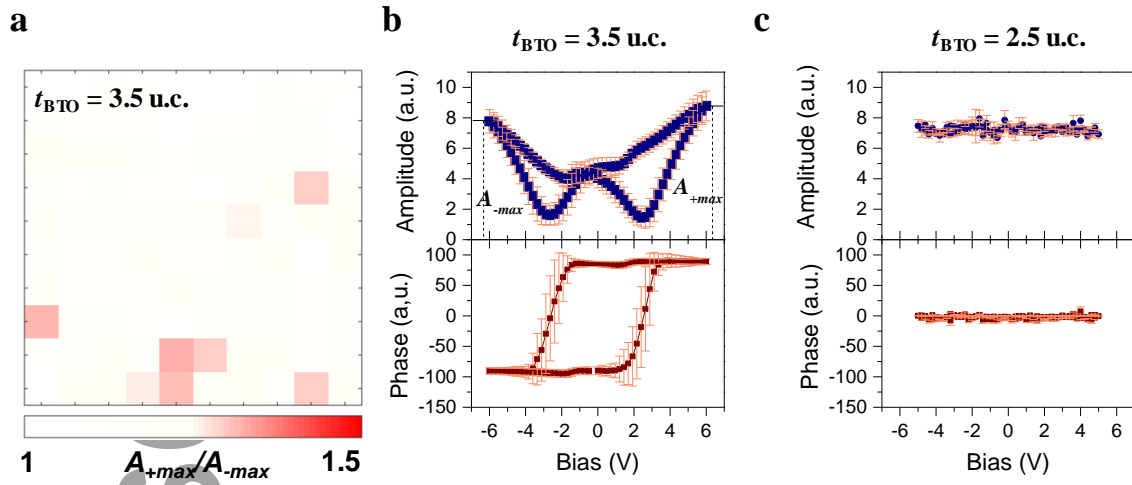
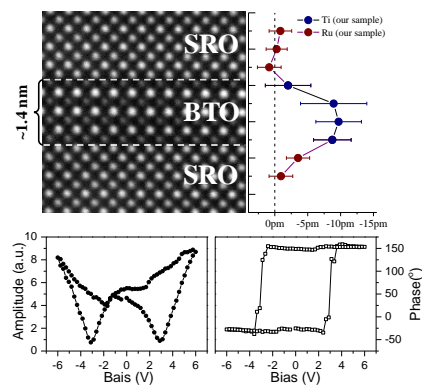


Figure 3. a) Color map of A_{+max}/A_{-max} for the SRO/BTO/SRO capacitor with $t_{BTO} = 3.5$ u.c. and with $P_{O_2} = 5$ mTorr. b) Averaged PFM amplitude and phase hysteresis loops measured at 10×10 different positions in a single capacitor. The error bar indicates the standard deviation of the measured loops. c) Averaged PFM amplitude and phase hysteresis loops of the SRO/BTO/SRO capacitor with $t_{BTO} = 2.5$ u.c..

Table of Contents

Ferroelectric SrRuO₃/BaTiO₃/SrRuO₃ capacitors with atomically-controlled and sharp interfaces are fabricated by pulsed laser deposition by adjusting the growth conditions and altering the thermodynamic surface stability of BaTiO₃. The interface atomic structure is designed to have a symmetric SrO-TiO₂ atomic sequence at the top and bottom interface, and the resulting ferroelectric capacitor exhibits a robust ferroelectricity down



to a thickness of ~1.4 nm.

Interface engineering, ferroelectric critical thickness, ferroelectricity, BaTiO₃

Y. J. Shin, Y. Kim, S. -J. Kang, H. -H. Nahm, P. Murugavel, J. R. Kim, M. R. Cho, L. Wang, S. M. Yang, J. -G. Yoon, J. -S. Chung, M. Kim, H. Zhou, S. H. Chang*, T. W. Noh*

Interface control of ferroelectricity in a SrRuO₃/BaTiO₃/SrRuO₃ capacitor and its critical thickness

This article is protected by copyright. All rights reserved.

Author Manuscript

This article is protected by copyright. All rights reserved.